Supporting online materials for

A metal-free and flexible supercapacitor based on redox-active lignin functionalized graphene hydrogel

Fengfeng Li, Xiluan Wang * and Runcang Sun *

Beijing Key Laboratory of Lignocellulosic Chemistry, Beijing Forestry University, Beijing, 100083, P. R. China.

Corresponding author: Tel: +86-10-62336903; Fax: +86-10-62336903

E-mail address: wangxiluan@bjfu.edu.cn; rcsun3@bjfu.edu.cn

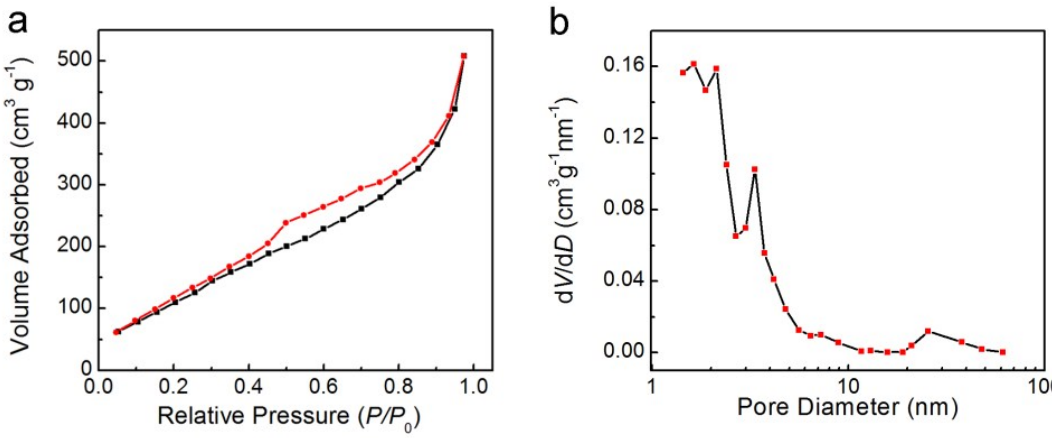

Figure S1. (a) Nitrogen adsorption-desorption isotherm and (b) pore size distribution of LS-GH calculated by Barrett-Joyner-Halenda method in Nitrogen adsorption.

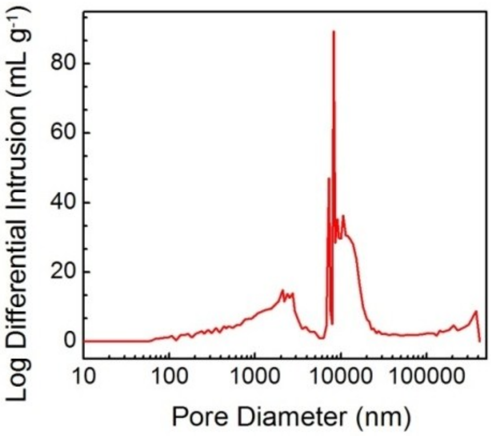

Figure S2. Statistical pore size distribution of LS-GH calculated by mercury intrusion porosimetry method.

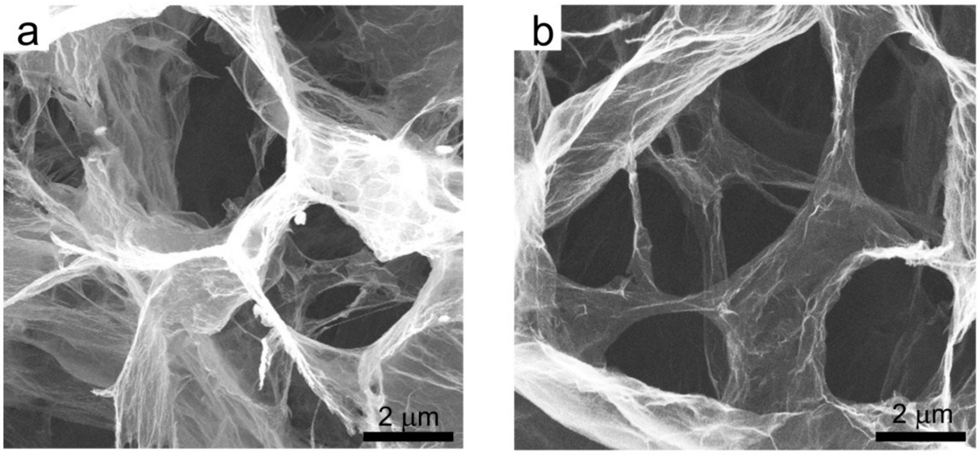

Figure S3. SEM images of freeze-dried samples of GH (a) and LS-GH (b).

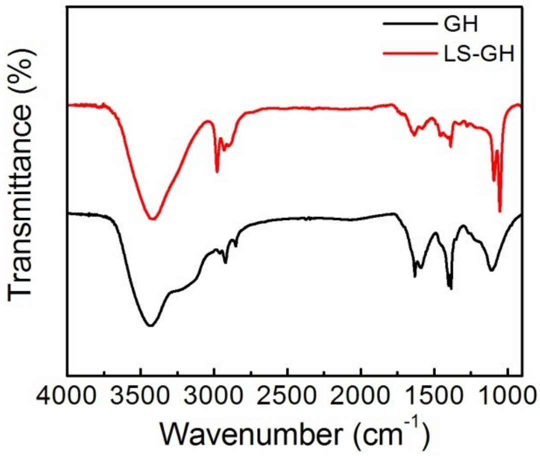

Figure S4. FTIR spectra of GH and LS-GH.

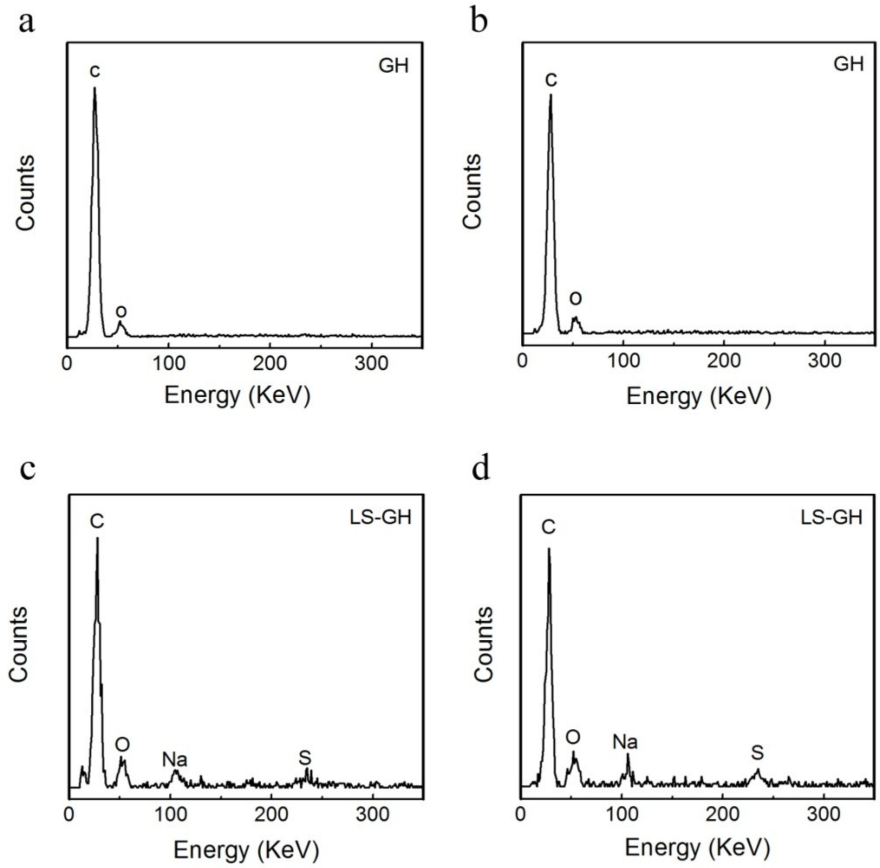

Figure S5. EDX spectra of GH (a, b) and LS-GH (c, d) in arbitrary positions.

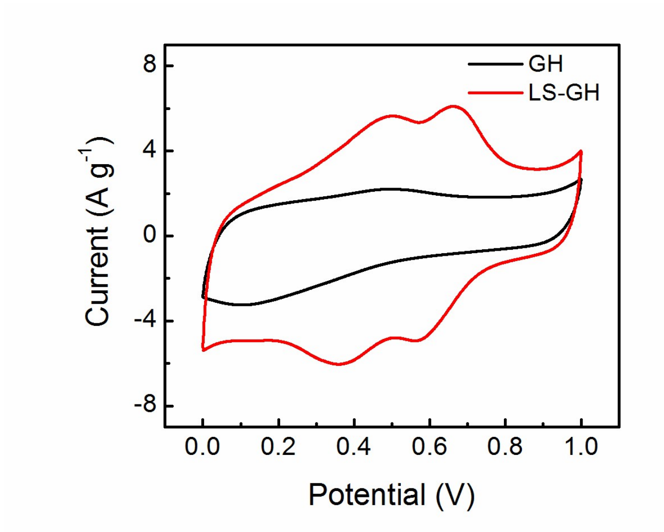

Figure S6. CV profiles of LS-GH and GH at a scan rate of 5 mV s^{-1} in a three-electrode configuration.

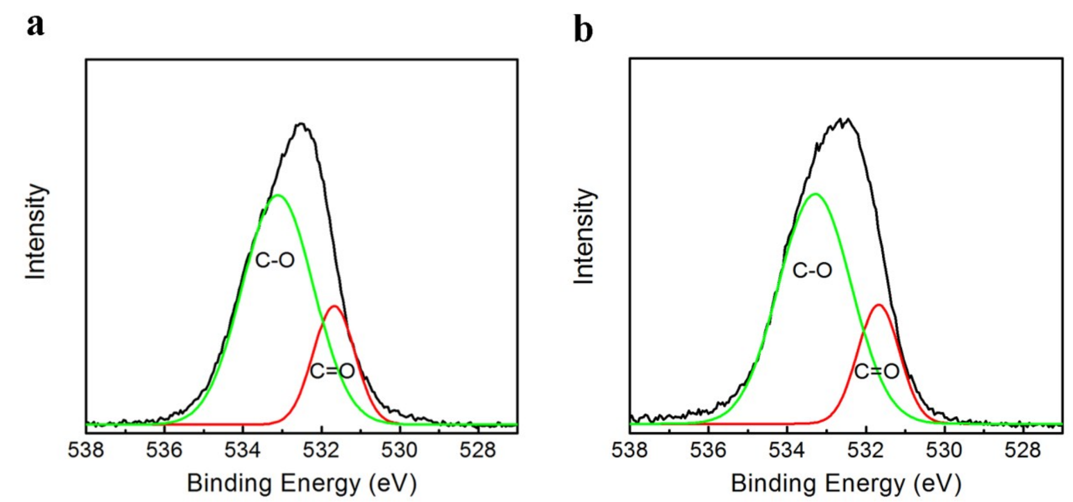

Figure S7. High-resolution XPS spectra of O 1s peaks for GH before (a) and after (b) charging.

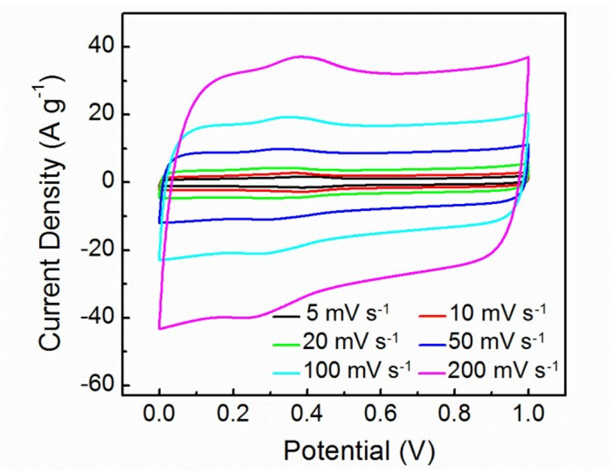

Figure S8. CV curves of LS-GH based symmetric supercapacitor in 1 M H_2SO_4 aqueous electrolyte at various scan rates ranging from 5 to 200 mV s^{-1}.

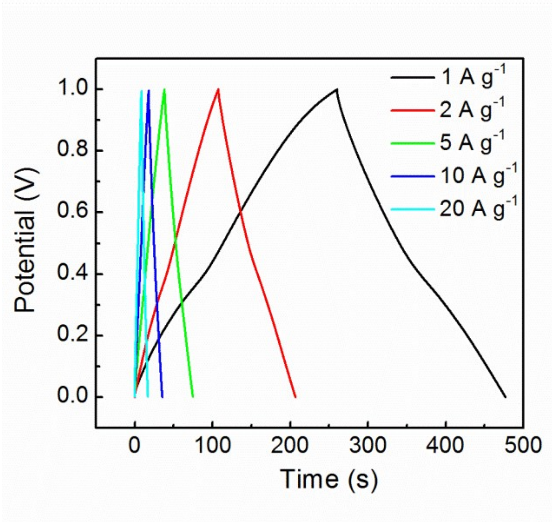

Figure S9. GC curves LS-GH based symmetric supercapacitor in 1 M H_2SO_4 aqueous electrolyte at different current densities ranging from 1 to 20 A g^{-1}.

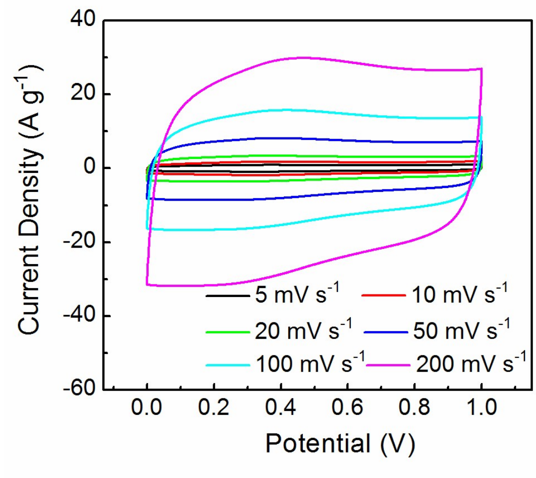

Figure S10. CV curves of LS-GH based flexible solid-state supercapacitor in PVA-H_2SO_4 gel electrolyte at the scan rate ranging from 5 to 200 mV s^{-1}.

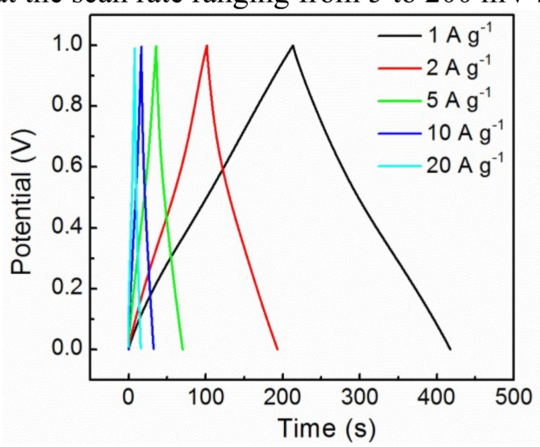

Figure S11. GC curves of LS-GH based flexible solid-state supercapacitor in PVA-H_2SO_4 gel electrolyte at the current density ranging from 1 to 20 A g^{-1}.

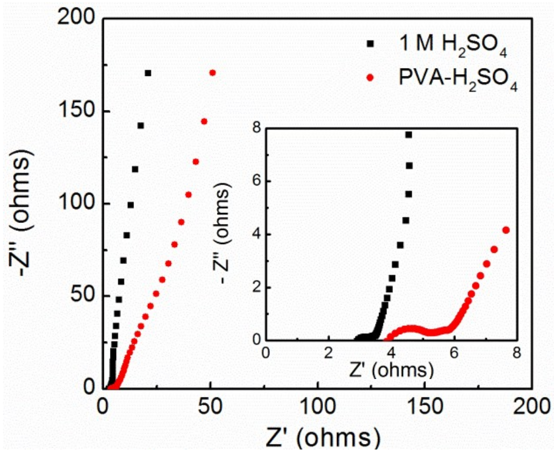

Figure S12. Nyquist plots of LS-GH based supercapacitor in aqueous H_2SO_4 and PVA-H_2SO_4 gel electrolyte.

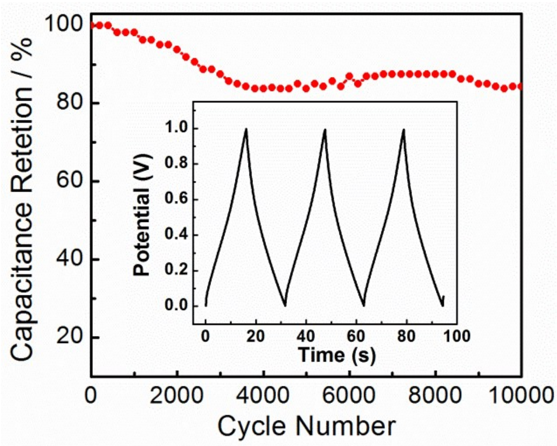

Figure S13. Cycling stability of the LS-GH based flexible solid-state supercapacitor in PVA-H_2SO_4 gel electrolyte at a current density of 10 A g^{-1}.

Table S1. Elemental analysis of the GH and LS-GH samples.

Sample	C	H	O	N	S
GH	77.85	1.25	20.33	0.14	0.43
LS-GH	70.37	2.24	25.91	0.25	1.23

Table S2. Capacitive performances of reported supercapacitors based on 3D graphene electrode materials in aqueous electrolyte.

Electrode materials	Current density or Scan rate	Specific capacitance	Cycling stability	Reference
LS-GH	1 A g^{-1}	432 F g^{-1}	98.8% (2000) 90% (10000)	This work
Graphene hydrogel	1 A g^{-1}	220 F g^{-1}	92% (2000)	13
MnO_2/graphene hydrogel	1 A g^{-1}	242 F g^{-1}	89.4 (1000)	21
MnO_2/graphene foam	1 A g^{-1}	422.5 F g^{-1}	None	16
TiO_2/graphene hydrogel	0.5 A g^{-1}	206.7 F g^{-1}	96.4% (150)	20
RuO_2/graphene hydrogel	1 A g^{-1}	345 F g^{-1}	None	S1
VO_2/graphene hydrogel	1 A g^{-1}	426 F g^{-1}	92% (5000)	S2
Nitrogen doped graphene/Fe_3O_4 aerogel	5 mV s^{-1}	386 F g^{-1}	97% (1000)	S3
Carbon nanotube spaced graphene aerogel	2.5 A g^{-1}	245.5 F g^{-1}	97% (2000)	40

Electrode materials	Current density or Scan rate	Specific capacitance	Cycling stability	Reference
3D hollow balls of graphene/polyaniline hybrid	1 A g^{-1}	331 F g^{-1}	86% (500)	S4
Nitrogen and boron co-doped graphene aerogel	1 mV s^{-1}	239 F g^{-1}	~100% (1000)	48
Hydroquinone functionalized graphene hydrogel	1 A g^{-1}	441 F g^{-1}	86% (10000)	11
Aminoanthraquinone functionalized graphene hydrogel	0.3 A g^{-1}	258 F g^{-1}	None	S5
Polypyrrole/graphene foam	1.5 A g^{-1}	350 F g^{-1}	None	S6
Polypyrrole/graphene hydrogel	10 mV s^{-1}	375 F g^{-1}	87% (4000)	S7
3D porous graphene/polyaniline film	0.5 A g^{-1}	385 F g^{-1}	88% (5000)	S8

Table S3. Capacitive performances of reported flexible solid-state supercapacitors based on 3D graphene electrode matrials in PVA-H_2SO_4 gel electrolyte.

Electrode materials	Current density or Scan rate	Specific capacitance	Cycling stability	Reference
LS-GHs	1 A g^{-1}	408 F g^{-1}	84% (10000)	This work
Graphene hydrogel	1 A g^{-1}	186 F g^{-1}	91.6% (10000)	10
Hydroquinone functionalized graphene hydrogel	1 A g^{-1}	412 F g^{-1}	87% (10000)	46
3D hollow balls of graphene/polyaniline hybrid	1 A g^{-1}	182 F g^{-1}	81.8% (500)	S4
3D nitrogen and boron co-doped graphene aerogel	5 mV s^{-1}	62 F g^{-1}	None	48
Mesoporous carbon/graphene aerogel	5 mV s^{-1}	44.3 F g^{-1}	92.6% (1000)	50
MoO_3 wrapped graphene framework	0.5 A g^{-1}	404 F g^{-1}	80% (5000)	49
ZIF-derived nitrogen doped carbon/3D graphene framework	5 mV s^{-1}	53 F g^{-1}	92% (1000)	S9
3D MnO_2/graphene foam	0.5 A g^{-1}	69.4 F g^{-1}	84.4% (10000)	16
Cellulose nanofiber/graphene aerogel	5 mV s^{-1}	207 F g^{-1}	99.1% (5000)	S10

Supplementary References

S1 Y. Y. Yang, Y. R. Liang, Y. D. Zhang, Z. Y. Zhang, Z. M. Li, Z. G. Hu, *New J. Chem.*, 2015, **39**, 4035–4040.

S2 H. W. Wang, H. Yi, X. Chen, X. F. Wang, *J. Mater. Chem.*, *A*, 2014, **2**, 1165–1173.

S3 X. Y. Zhang, S. H. Sun, X. J. Sun, Y. R. Zhao, L. Chen, Y. Yang, W. Lü, D. B. Li, *Light: Sci. Appl.*, 2016, **5**, e16130.

S4 N. B. Trung, T. Van Tam, H. R. Kim, S. H. Hur, E. J. Kim, W. M. Choi, *Chem. Eng. J.*, 2014, **255**, 89–96.

S5 Q. Wu, Y. Q. Sun, H. Bai, G. Shi, *Phys. Chem. Chem. Phys.*, 2011, **13**, 11193–11198.

S6 Y. Zhao, J. Liu, Y. Hu, H. H. Cheng, C. G. Hu, C. Jiang, L. Jiang, A. Y. Cao, L. T. Qu, *Adv. Mater.*, 2013, **25**, 591–595.

S7 F. Zhang, F. Xiao, Z. H. Dong, W. Shi, *Electrochim. Acta*, 2013, **114**, 125–132.

S8 Y. N. Meng, K. Wang, Y. J. Zhang, Z. X. Wei, *Adv. Mater.*, 2013, **25**, 6985–6990.

S9 L. Wan, J. Wei, Y. Liang, Y. X. Hu, X. F. Chen, E. Shamsaei, R. W. Ou, X. W. Zhang, H. T. Wang, *RSC Adv.*, 2016, **6**, 76575–76581.

S10 K. Z. Gao, Z. Q. Shao, J. Li, X. Wang, X. Q. Peng, W. J. Wang, F. J. Wang, *J. Mater. Chem. A*, 2013, 1, 63–67.